Electronic Supplementary Material (ESI) for Journal of Materials Chemistry C.

Plasmonic $Cu_{1.8}S$ nanocrystals as saturable absorbers for passively Q-switched erbium-doped fiber lasers

Mingyi Liu[a], Donglei Zhou[a], Zhixu Jia[a], Zhenrui Li[a], Nan Li[a], Siqing Li[a], Zhe Kang[b], Jun Yi[c], Chujun Zhao[c], Guanshi Qin*[a], Hongwei Song[a], and Weiping Qin*[a]

a. State Key Lab on Integrated Optoelectronics, College of Electronic Science &Engineering, Jilin University, Changchun 130012, China. E-mail: qings@jlu.edu.cn, wpqin@jlu.edu.cn; Fax: +86 4318516 8241; Tel: +86 431 8516 8325.

b. Changchun Observatory National Astronomical Observatories, CAS, Changchun 130117.

c. Key Laboratory for Micro-/Nano-Optoelectronic Devices of Ministry of Education, School of Physics and Electronics, Hunan University, Changsha 410082, China.

Supplementary Information

1. Synthesis and characterization of $Cu_{1.8}S$ NCs

1.1 Synthesis of $Cu_{1.8}S$ NCs[1-5]

Copper precursor was prepared by mixing CuCl (0.01 mol) with a mixture of 4 mL oleic acid(OA) and 5 mL oleylamine(OAm) at 130°C under continuous stirring. Then, the as-prepared copper precursor was cooled to room temperature. Sulfur precursor was prepared in a three necked flask by dissolving sulfur powder (0.01 mol) into 40 mL ODE at 200 °C under continuous stirring. Subsequently, the temperature of sulfur solution was set to 180 °C, followed by a swift injection of copper precursor. $Cu_{1.8}S$ NCs were obtained under the above conditions. After cooling down to room temperature naturally, the obtained products were washed with cyclohexane and ethanol and centrifuged under the 5000 revolutions per minute for 10 min for three times, respectively. Then the obtained samples were dried at 70 ℃ for 24 h in a drying oven.

1.2 Characterizations of $Cu_{1.8}S$ NCs

1.2.1 Characterizations of $Cu_{1.8}S$ NCs powder

The elements of Cu and S in our materials were measured by using EDX. EDX spectrum was recorded to confirm the elemental compositions of the resulting sample. The result indicates the coexistence of Cu^{+} and Cu^{2+} in the $Cu_{2-x}S$ NPs. The atomic ratios of Cu to S were determined to be 1.82 for $Cu_{2-x}S$ NPs and the atomic ratios of Cu and S were shown in the inset of Fig. S1.

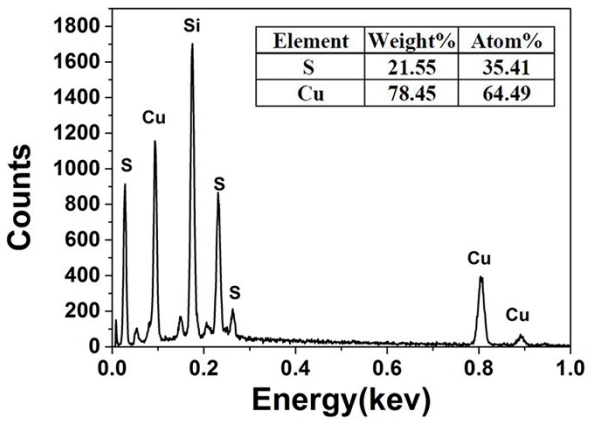

Figure S1. The result spectrum of EDX. Inset: the atom proportion of the Cu and S.

We dispersed as-prepared $Cu_{1.8}S$ NCs in cyclohexane, and coated them on a silica glass. After drying at room temperature for about 2 hours, and then measured by using an ultraviolet-visible near-infrared spectrophotometer (UV-3600 Shimadzu). The $Cu_{1.8}S$ NCs only have one absorption peak at 1218 nm as shown in Fig. S2.

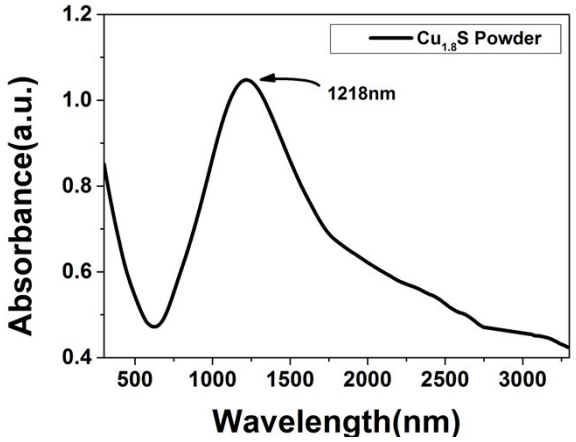

Figure S2. The absorption spectrum of the $Cu_{1.8}S$ NCs powder with the central wavelength at about 1218nm.

1.2.2 Characterizations of $Cu_{1.8}S$ NCs film

Figure S3 shows the absorption spectrum of the $Cu_{1.8}S$ NCs SA film by removing the background absorption (absorption of the NaCMC film).

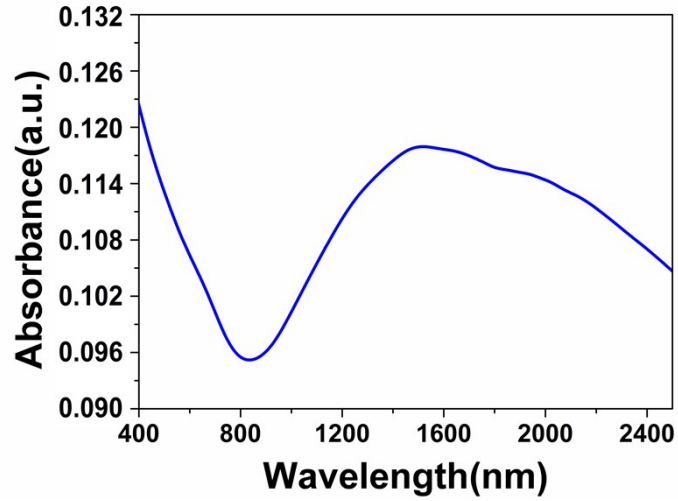

Figure S3. Absorption spectrum of the $Cu_{1.8}S$ NCs SA film by removing the background absorption (absorption of the NaCMC film).

1.2.3 The saturable absorption properties of the $Cu_{1.8}S$ SA films

Figure S4 shows the measured results of $Cu_{1.8}S$ NCs films, which clearly exhibit the feature of saturable absorption. The saturation power density and modulation depth increased with an increase of the concentration of the $Cu_{1.8}S$ NCs.

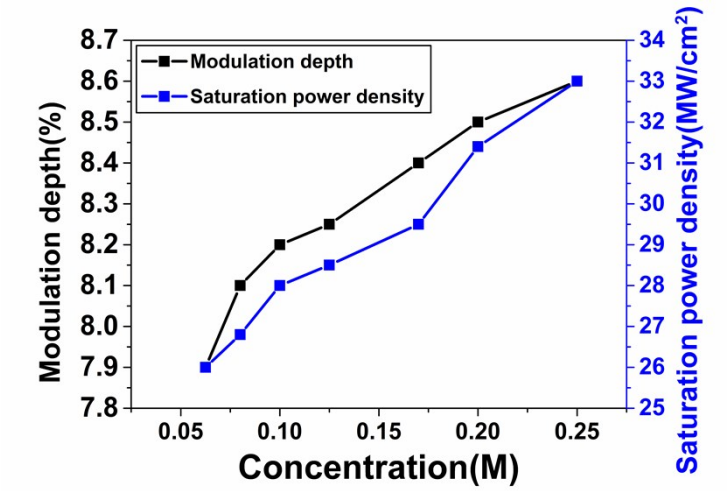

Figure S4. Dependence of the saturable absorption properties of the $Cu_{1.8}S$ SA films on the concentration of the $Cu_{1.8}S$ NC.

2. Calculation of hole density[6, 7]

Previously studies show that the LSPR frequency of noble metal nanocrystal was decided by the dielectric function ε, and dielectric constant ε_m. The dipole polarizability, α, of the small spherical nanoparticle that the size was much smaller than the wavelength of the light is given as the following equation:

$$\alpha = 3\varepsilon_0 V\left(\frac{\varepsilon - \varepsilon_m}{\varepsilon + 2\varepsilon_m}\right) \quad (1)$$

In the equation, *v* is the nanoparticle volume and ε_0 is the free space permittivity. Such a nanoparticle exhibits a dipolar LSPR when the denominator reduces as follows.

$$\varepsilon_r = -2\varepsilon_m \quad (2)$$

Where ε_0 represent the real part of ε, expressed as a function of the frequency of light ω by the Drude model:

$$\varepsilon_r = 1 - \frac{\omega_p^2}{\omega^2 + \gamma^2} \quad (3)$$

Here ω_p is the bulk plasma oscillation frequency associated with the free carriers and γ is their bulk collision frequency. From (2) and (3) we get the frequency ω_{sp} at which the resonance condition described by equation (2) is satisfied:

$$\omega_{sp} = \sqrt{\frac{\omega_p^2}{1 + 2\varepsilon_m} - \gamma^2} \quad (4)$$

ω_{sp} represents the LSPR energy and represents the line width of the plasmon resonance band. From equation (4) we estimate the plasmon wavelength. We assume that the dielectric function of copper sulphide in the NIR region is dominated by free carriers, because the bandgap contribution can be neglected.

The bulk plasma frequency ω_p depends on the density N_h of free carriers (holes) as:

$$\omega_p = \sqrt{\frac{N_h e^2}{\varepsilon_0 m_h}} \quad (5)$$

Where m_h is the hole effective mass, approximated as $0.8m_0$, where m_0 is the electron mass. The spectrum in Fig. S2 shows that the central wavelength of the $Cu_{1.8}S$ NCs powder is about 1218 nm. From equation (5), N_h is estimated to be 1.53×10^{21} cm^{-3}. From previous studies on the copper chalcogenide and the LSPR, the hole

density of ~10^{21}cm^{-3} is a typical magnitude in the copper sulphide. The above results show that the N_h is reasonable enough to support a LSPR and the LSPR is the main mechanism responsible for the absorption in the $Cu_{1.8}S$ NCs.

3. Z-scan data[8-10]

The measured data was fitted by using the following formula. :

$$T = [1 - \frac{\alpha_0 L I_s}{I_s + I_0/(1 + z^2/z_0^2)} - \beta L I_0/(1 + z^2/z_0^2)]/(1 - \alpha_0 L) \quad (6)$$

Where L is the sample length, I_0 is the focus light intensity, I_S is the saturable intensity, β is the nonlinear absorption coefficient, and the Z_0 is diffraction length of the beam. It can be seen that the fitting curves fit the saturable absorption data perfectly. These results show that $Cu_{1.8}S$ NCs have nonlinear saturable absorption at 1560nm and the β value of $Cu_{1.8}S$ NCs at 1560 nm is about 4.5×10^{-6}cm/w.

4. Synthesis and characterization of gold nanorods (GNRs)

4.1. Synthesis and characterization of GNRs

In our experiment, GNRs were synthesized by the seed-mediated growth method. The seed solution was synthesized based on the previously published paper[11-13]. A 5 ml of 0.034 mol/L $HAuCl_4$ aqueous solution was mixed with 20 ml of 2 mol/L Hexadecyltrimethyl ammonium bromide (CTAB) solution in a beaker. The mixture solution was stirred at 60 ℃ for about 15 min. Then 1 ml of 0.0005 mol/L freshly $NaBH_4$ solution was injected into the above seed solution. The color of the solution was changed from yellow to dark brown immediately. The seed solution was kept at 60℃ for 1 hour and then used for the synthesis of GNRs. The growth solution was prepared by mixing 0.03 mol CTAB, 0.0007 mol ortho-hydroxybenzoic acid, and 31.25 ml deionized water in a flask. After mixing, 1ml of 0.004 mol/L $AgNO_3$ solution, 0.156 ml of 0.00065 mol/L L-ascorbic acid aqueous solution and 31.25 ml of 0.03375 mol/L $HAuCl_4$ aqueous solution was added into the growth solution. The color of the solution was turned to orange at once and then became colorless. 0.226 ml of 12 mol/L HCl solution was used to reduce the PH value below 7.0. Finally, 0.2 ml of seed solution was injected into the growth solution to initiate the growth of the GNRs. The final solution was kept at room temperature for 8 hours and GNRs solution was obtained.

Figure S5 (a) shows the transmission electron microscopy (TEM, Hitachi H-600) image of prepared GNRs. The rod-shape nanoparticles were obtained, only a small amount of the spherical nanoparticles existed in the GNRs sample. The diameters of these GNRs were about ~10nm and the aspect ratios were in a range of 4.5~8, as shown in Fig. S5 (b). Most of GNRs (~70%) have aspect ratios of 6~7. The inset of Fig. S5 (a) shows the photograph of the aqueous solution of GNRs.

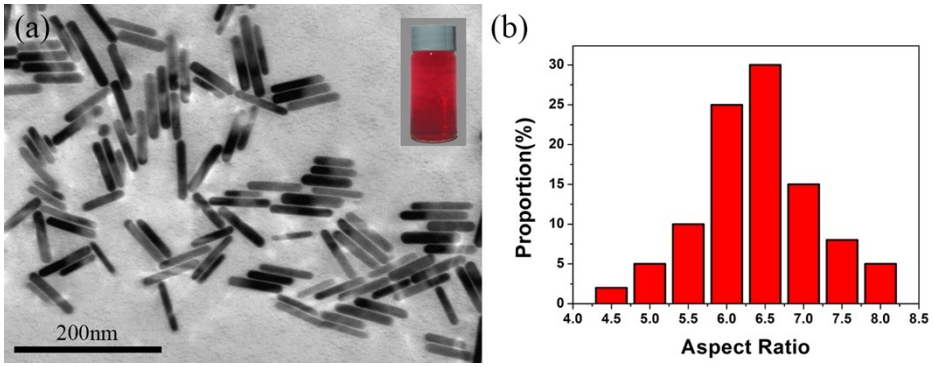

Figure S5. (a) TEM image of as-prepared GNRs and the picture of the GNRs solution. (b) Aspect ratio proportion of GNRs.

4.2. Synthesis and characterization of GNRs-NaCMC film

The GNRs solution and carboxymethylcellulose sodium (NaCMC) aqueous solution were mixed to form GNRs-NaCMC solution. Then the GNRs film was formed by casting the mixed solution onto a flat silica substrate, followed by a slow drying at room temperature. Figure S6 showed the absorption spectrum of the GNRs-NaCMC film. It shows that the film has a LSPR absorption peak at 1100 nm.

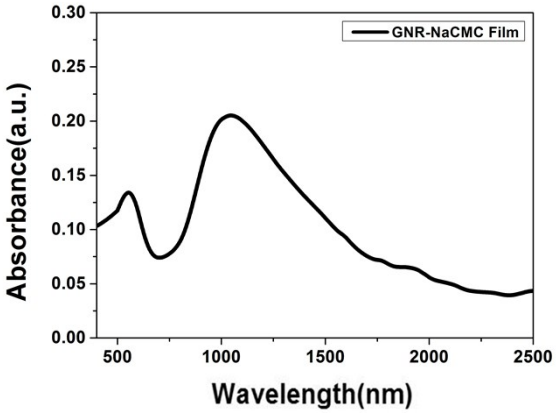

Figure S6. The absorption spectrum of GNRs-NaCMC Film

5. Long-term stability of $Cu_{1.8}S$ NCs as saturable absorbers

Long-term stability is a key issue for Q-switched lasers based on the saturable absorbers. To confirm the long-term stability of $Cu_{1.8}S$ NCs as SAs, we measured the emission spectrum of the Q-switched laser based on $Cu_{1.8}S$ NCs SA every 15 min for 2 hours. The measured emission spectra are shown in Fig. S7. It can be seen that the emission spectrum of the Q-switched laser was not changed. These results showed that the $Cu_{1.8}S$ NCs SA is stable for constructing Q-switched lasers.

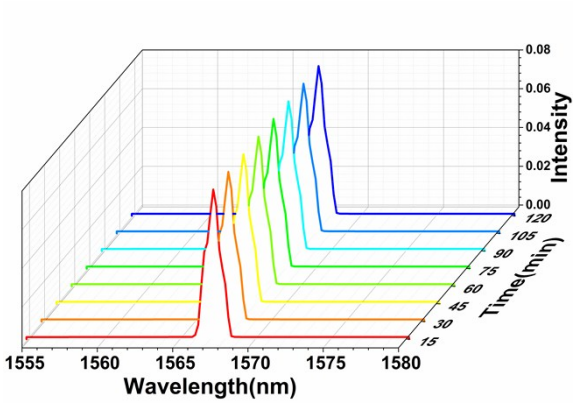

Figure S7. The measured emission spectra of the Q-switched laser based on the $Cu_{1.8}S$ NCs SA.

1. Y. Ke, State University of New York at Buffalo, ProQuest Dissertations Publishing, 2015, **No. 1594737**.
2. B. Li, Y. Xie and Y. Xue, J Phys. Chem. C, 2007, **111**, 12181-12187.
3. X. Li, A. Tang, L. Guan, H. Ye, Y. Hou, G. Dong, Z. Yang and F. Teng, Rsc Adv., 2014, **4**, 54547-54553.
4. L. Liu, H. Zhong, Z. Bai, T. Zhang, W. Fu, L. Shi, H. Xie, L. Deng and B. Zou, Chem. Mater., 2013, **25**, 4828-4834.
5. J. Mou, C. Liu, P. Li, Y. Chen, H. Xu, C. Wei, L. Song, J. Shi and H. Chen, Biomaterials, 2015, **57**, 12-21.
6. P. K. Jain, X. Huang, I. H. El-Sayed and M. A. El-Sayed, Accounts Chem. Res., 2008, **41**, 1578-1586.
7. Z. Yixin, P. Hongcheng, L. Yongbing, Q. Xiaofeng, Z. Junjie and B. Clemens, Chem. Inform., 2009, **131**, 4253-4261.
8. E. Garmire, J Selected Topics Quan. Elec., 2000, **6**, 1094-1110.

9. J. Wang, Y. Hernandez, M. Lotya, J. N. Coleman and W. J. Blau, Adv. Mater., 2009, **21**, 2430–2435.
10. H. Zhang, S. Lu, J. Zheng, J. Du, S. Wen, D. Tang and K. Loh, Opt. Express, 2014, **22**, 7249-7260.
11. Z. Kang, X. Gao, L. Zhang, Y. Feng, G. Qin and W. Qin, Opt. Mater. Express, 2015, **5**, 794-801.
12. Z. Kang, X. Guo, Z. Jia, Y. Xu, L. Liu, D. Zhao, G. Qin and W. Qin, Opt. Mater. Express, 2013, **3**, 1986-1991.
13. Z. Kang, Y. Xu, L. Zhang, Z. Jia, L. Liu, D. Zhao, Y. Feng, G. Qin and W. Qin, Appl. Phys. Lett., 2013, **103**, 041105-1-4.